

## Particle–wall collisions in a viscous fluid

By G. G. JOSEPH<sup>1</sup>, R. ZENIT<sup>2</sup>, M. L. HUNT<sup>1</sup>  
AND A. M. ROSENWINKEL<sup>1</sup>

<sup>1</sup>Division of Engineering and Applied Sciences, California Institute of Technology, Pasadena,  
CA 91125, USA

<sup>2</sup>Instituto de Investigaciones en Materiales, Universidad Nacional Autónoma de México,  
México D.F. 04510, México

(Received 18 July 2000 and in revised form 24 October 2000)

This paper presents experimental measurements of the approach and rebound of a particle colliding with a wall in a viscous fluid. The particle's trajectory was controlled by setting the initial inclination angle of a pendulum immersed in a fluid. The resulting collisions were monitored using a high-speed video camera. The diameters of the particles ranged from 3 to 12 mm, and the ratio of the particle density to fluid density varied from 1.2 to 7.8. The experiments were performed using a thick glass or Lucite wall with different mixtures of glycerol and water. With these parameters, the Reynolds number defined using the velocity just prior to impact ranged from 10 to approximately 3000. A coefficient of restitution was defined from the ratio of the velocity just prior to and after impact.

The experiments clearly demonstrate that the rebound velocity depends on the impact Stokes number (defined from the Reynolds number and the density ratio) and weakly on the elastic properties of the material. Below a Stokes number of approximately 10, no rebound of the particle occurred. For impact Stokes number above 500 the coefficient of restitution appears to asymptote to the values for dry collisions. The coefficients of restitution were also compared with previous experimental studies. In addition, the approach of the particle to the wall indicated that the particle slowed prior to impacting the surface. The distance at which the particle's trajectory varied due to the presence of the wall was dependent on the impact Stokes number. The particle surface roughness was found to affect the repeatability of some measurements, especially for low impact velocities.

---

### 1. Introduction

In many particulate multi-phase flows particle–particle and particle–wall collisions play an important role in the dynamic behaviour of the mixture. In addition, any modelling of these flows requires a detailed understanding of the mechanics of individual collisions. In dry granular flows where the effect of the interstitial fluid is negligible, the amount of energy dissipation due to the inelasticity of the contacts is often characterized by a coefficient of restitution, defined by the ratio of the rebound to impact velocity. In discrete element simulations of dry flows, the coefficient of restitution is used as an input parameter to model the collision of two particles or the collision between a particle and a wall. In general, a constant coefficient of restitution is assumed, although it is possible to allow the coefficient to vary. The values, however, are often obtained from idealized experiments that may not be representative of the conditions encountered in applications.

In a similar manner an effective coefficient of restitution may be useful in describing a collision in which the effects of the interstitial fluid are important. Such a coefficient must account for the viscous dissipation and the kinetic energy needed to displace the fluid between the surfaces in addition to the inelasticity of the contact. This information would be useful for simulations of liquid–solid flows, such as found in the recent numerical simulations by Hu (1996) and Glowinski *et al.* (1999). For example, in these simulations, the motion of the interstitial fluid is calculated directly; however, the solid surfaces are not allowed to touch because contact would break the lattice modelling of the fluid. Hence, a repulsive force between the particles is incorporated to prevent contact between surfaces.

The problem of a sphere of mass  $m$  moving toward a surface or toward another sphere in a fluid has been studied by many researchers. Brenner (1961) analysed the problem of a sphere moving towards a wall at small Reynolds number ( $Re = \rho_f v_0 d / \mu$ , where  $\rho_f$  is the fluid density,  $v_0$  is the approach velocity,  $d$  is the reduced particle diameter, and  $\mu$  is the fluid dynamic viscosity), and found that the hydrodynamic force diverges as the gap separation,  $h$ , tends to zero; therefore, in the absence of elasticity of the particles or of the fluid, a rebound of the particles would not be possible. In a later study by Davis, Serayssol & Hinch (1986), the particle surfaces were allowed to deform elastically due to the increase in hydrodynamic pressure. As a result, some of the incoming kinetic energy of the particle is stored as elastic strain energy. This strain energy is released after the particle comes to rest, resulting in a rebound of the particles. However, since fluid always remains in the gap between the particles, physical contact between surfaces does not occur. The results from their analysis showed that the maximum particle deformation and the rebound of the particle after collision (measured in terms of the ratio of rebound velocity  $v_r$  to approach velocity  $v_0$ ), depend on the particle Stokes number,  $St = mv_0 / 6\pi\mu a^2 = (1/9)Re(\rho_p/\rho_f)$  and an elasticity parameter,  $\epsilon = 40\mu w_0 a^{3/2} / x_0^{5/2}$ , where  $\theta$  is defined as  $\theta = (1 - v_1^2) / \pi E_1 + (1 - v_2^2) / \pi E_2$  and depends on the Young's modulus and Poisson's ratio of the two bodies;  $x_0$  is the position within the gap between the undeformed surfaces at which the velocity is  $v_0$ , and  $a = d/2$  is the particle radius. Since their analysis assumes that the Reynolds number based on the distance  $x_0$  is much less than one, the results are independent of the fluid density.

Barnocky & Davis (1989) extended the analysis of Davis *et al.* (1986) to include the variation of the density and viscosity with pressure. They observed that an increase in density of the fluid during compression could enhance the rebound of a impacting particle, even when the particle was completely rigid. The increase in viscosity with pressure results in the fluid behaving like an elastic solid, significantly affecting the deformation of an elastic particle and enhancing the rebound of the particle from a surface. The perturbation analysis by Kytomaa & Schmid (1992) examined the effect of fluid compressibility on a collision between two particles by assuming that the solid is incompressible. Using a linear representation for the density dependence on pressure, the particle does not rebound. However, they conjecture that a nonlinear dependence of the density on pressure might result in a rebound of the particle even when the particles were incompressible.

As pointed out by Smart & Leighton (1989), the thickness of the lubrication layer between two colliding particles is very small, and may be on the order of the size of the surface roughness. Hence, they argued that surface roughness may have a significant impact on models based on perfectly smooth particles because contact may occur through microscopic surface imperfections.

Experimentally, Lundberg & Shen (1992) and Barnocky & Davis (1988) obtained

measurements of the coefficient of restitution for the case when a drop of fluid was placed in the gap between the sphere and a surface. The results by Barnocky & Davis (1988) show a critical Stokes number above which rebound occurs. For smooth surfaces, this critical Stokes number varies from approximately 0.25 to 4.

Three experimental studies examined the rebound of a particle falling at its terminal velocity and impacting a submerged surface. McLaughlin (1968), Gondret *et al.* (1999) and Gondret, Lance & Petit (2000) dropped particles in a tank immersed in various viscous fluids to study the transition from arrest to rebound. McLaughlin used steel spheres of different diameters and glycerol–water mixtures and a thick steel anvil as a target. In Gondret *et al.* (1999), glass beads or steel spheres were used in either water or glycerol or silicone oil; the surface was a relatively thin glass plate, twice as thick as the diameter of their largest particle. In the recent study by Gondret *et al.* (2000), the target surface was thicker and particles of tungsten carbide, stainless steel, soda glass, Teflon, Delrin, polyurethane, and nylon were used. In all studies, the authors observed that there was no rebound of the particle below a certain threshold. In Gondret *et al.* (1999), there was no rebound for a Stokes number of 12, but rebound did occur at  $St = 29$ , which was obtained with a steel ball falling in silicone oil. In McLaughlin, there was no rebound at  $St = 10$ , but there was rebound at  $St = 19$ . Neither McLaughlin (1968) nor Gondret *et al.* (1999) reported data for a Reynolds number from approximately 150 to 5000. As noted by McLaughlin, the motion of the falling particle was erratic due to the shedding of vortex rings in the wake of the sphere. In the later Gondret *et al.* (2000), measurements are reported for a range of Reynolds numbers of approximately 2 to 2000; no rebound is reported for  $St = 12$ , but rebound did occur at slightly higher values of Stokes number.

This paper presents the measured coefficients of restitution for particles immersed in water or in glycerol–water mixtures. The experimental arrangement is similar to that used by Zenit & Hunt (1999). In those experiments the objective was to measure the pressure impulse resulting from a particle collision. In the current study, the objective is to examine the approach and rebound trajectories. A simple pendulum experiment was used to produce controlled collisions for Reynolds numbers from 10 to 3000. The trajectories were measured using a high-speed video camera. Results are presented for a range of particle sizes and densities, for two different wall materials and for different fluids. These results are compared with the earlier studies. In addition, this study experimentally shows a deceleration of the particle prior to impact and the dependence of the rebound velocity on the surface roughness. These effects were not observed in the work by McLaughlin (1968) or Gondret *et al.* (1999, 2000).

## 2. Experimental setup and procedure

The experimental arrangement is shown in figure 1. A fine nylon string of diameter 0.075 mm was attached to a sphere that was positioned at an initial angle,  $\phi_i$ . A mechanism, consisting of a pair of nylon-lined tweezers and a lever, released the sphere from its initial position without rotation. The wall was positioned such that contact occurred at  $\phi = 0$ .

Five different particle types, with diameters ranging from 3 to 12 mm, were used in the experiments. The particle properties such as density, Young's modulus, Poisson's ratio, diameter, and sphericity,  $\varepsilon$  (defined for a given particle as the difference between the largest diameter and the smallest diameter, divided by the nominal diameter), are summarized in table 1. The particles include glass grinding beads, glass spheres, steel ball bearings, and nylon and Delrin spheres. The glass grinding beads are inexpensive

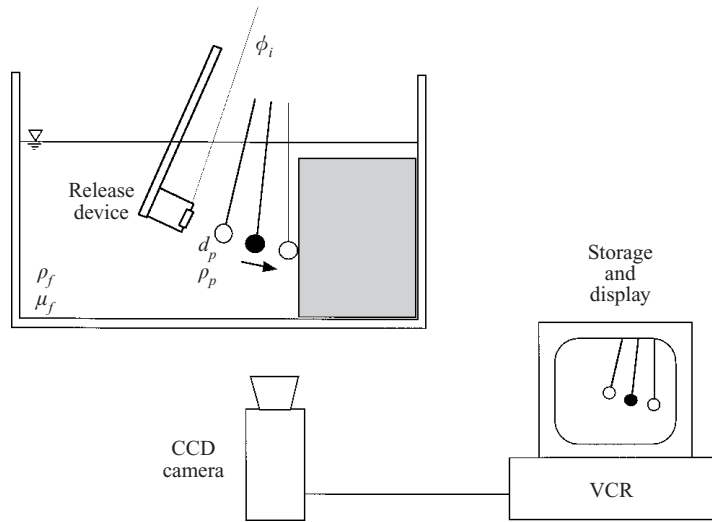


FIGURE 1. Schematic representation of the experimental setup. Note that the focal plane of the CCD camera is actually vertical and parallel to the plane of the pendulum.

Material	$d_p$ (mm)	$\varepsilon$	$\rho_p$ ( $\text{kg m}^{-3}$ )	$E$ (GPa)	$\nu$	$\sigma_s$ ( $\mu\text{m}$ )	$\lambda_p$ ( $\mu\text{m}$ )
Glass beads	3.0	0.0625	2540	60	0.23	0.1384	44.70
	4.1	0.0588	2540	60	0.23	0.0502	41.06
	6.0	0.0476	2540	60	0.23	0.0721	49.76
Glass sphere	6.35	0.0031	2540	60	0.23	0.1305	22.59
Steel	4.1–7.93	0.0024	7780	190	0.27	0.0236	48.04
Nylon	6.35	0.0031	1140	2.76	0.40	2.0114	41.86
Delrin	12.7	0.0039	1400	2.8	0.35	0.7960	101.49

TABLE 1. Properties of particles used in collision experiments.

and have a significant variation in particle diameter and a lower value of  $\varepsilon$ . The glass spheres have much tighter size tolerance, a consequence of having been ground into a spherical shape. The table also includes the root-mean-square surface height,  $\sigma_s$ , and the correlation distance,  $\lambda_p$ , measured from scanning electron microscopy images, which are discussed in § 4.1.

Mixtures of up to 75% glycerol in water were used as the surrounding fluid for all the performed experiments. The majority of the data presented in this paper were obtained with two different blocks of material: zerodur (a glass-like material) and Lucite. The properties of the blocks are given in table 2. The blocks were chosen so that their thickness,  $b$ , was much larger than the particle diameter (see Goldsmith 1960; Sondergaard, Chaney & Brennen 1990). For comparison, a thin 6.35 mm glass plate was also used. The surfaces were polished in order to minimize any effects of wall roughness in the experiments. Due to limitations in the size of the chamber of the scanning electron microscope used, it was not possible to measure the surface properties of the zerodur block. However, the analysis of a small sample from the Lucite block showed that the polished surfaces had a roughness comparable to that of the steel particles.

The motion of the sphere was filmed using a high-speed digital camera with framing

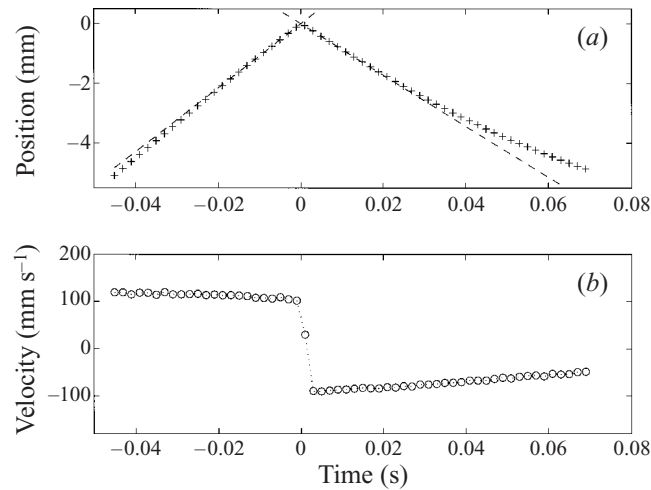


FIGURE 2. Particle position and velocity for a 6.35 mm glass particle released from an angle of  $12^\circ$  impacting the zerodur wall in water. For this collision, the coefficient of restitution is 0.8 ( $Re = 745$ ,  $St = 211$ ).

Material	$b$ (mm)	$\rho$ ( $\text{kg m}^{-3}$ )	$E$ (GPa)	$\nu$
Glass	6.35	2540	65	0.23
Zerodur	75	2530	91	0.24
Lucite	50	1100	40	0.32

TABLE 2. Properties of walls used in collision experiments.

rates up to 2000 frames per second for a full size image (520 pixels wide by 100 pixels high). The digital movie was then processed to determine the position of the centroid of the particle in each frame. Since the images were taken such that typically 160 pixels appeared across the diameter of the particle, the precision of the position could be determined within 0.3% of a particle diameter, corresponding to a resolution of one-half of a pixel.

Figure 2 is an example of the position–time and velocity–time plots recorded at 500 frames per second of a particle approaching the zerodur wall in water. The data correspond to a 6.35 mm diameter glass particle released from an initial angle of  $12^\circ$  supported by a line of length 10.5 cm. Two lines are drawn through the five data points before and after impact. For all of the data presented in this paper, line fits were done over five–ten points, depending on the framing rate. In all cases, the correlation coefficient of the line to the data had a value of 0.995 or higher, which is within the resolution of the measurement. The slopes of the fitted lines give the rebound and impact velocities ( $u_r$  and  $u_i$ ), which are used to calculate the coefficient of restitution for a normal impact,

$$e = -\frac{u_r}{u_i}.$$

The origin in the figure represents the point at which the particle reverses its direction of motion and is determined from the intersection of the approach and rebound line fits. The value of the position coordinate represents the gap between the particle

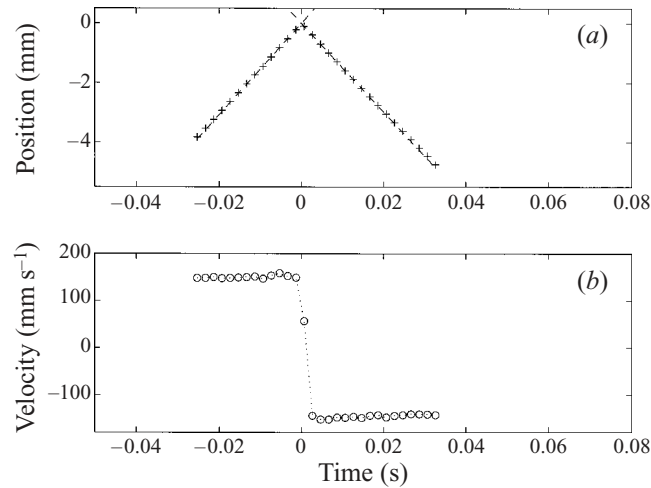


FIGURE 3. Particle position and velocity for a 6.35 mm glass particle released from an angle of  $12^\circ$  impacting the zerodur wall in air. For this collision, the coefficient of restitution is 0.968 ( $Re = 62.5$ ,  $St = 15000$ ).

and the wall. The velocity of the particle, shown in figure 2(b), is obtained from the discrete sampled position data using a first-order backward differencing scheme. For comparison, figure 3 shows similar position–time and velocity–time data for the same particle impacting the zerodur wall in air. When the particle is immersed in a liquid (figure 2), the trajectory shows a slight deceleration due to viscous drag as it approaches the wall, which is not observed in the collision in air (figure 3).

### 3. Results

#### 3.1. Dry coefficients of restitution

To assess the accuracy of the presented experimental setup and to provide a comparison base for the data, a series of measurements of the dry coefficient of restitution was obtained. In a dry collision the effect of the surrounding fluid is assumed to be negligible.

For impacts of glass or steel particles against the zerodur wall within a range of velocities of  $40\text{--}360\text{ mm s}^{-1}$ , the mean coefficient of restitution,  $\bar{e}$ , was  $0.97 \pm 0.02$ , which agrees with the values measured by Foerster *et al.* (1994). For the same particles and velocity range with the Lucite wall, the value was lower,  $\bar{e} = 0.92 \pm 0.03$ . For the collisions of nylon or Delrin particles, the value is approximately  $\bar{e} = 0.90 \pm 0.03$ , corresponding to a range of velocities of  $50\text{--}120\text{ mm s}^{-1}$ . This range of velocities for the glass and steel particles is less than the velocity corresponding to the fully plastic impact region for which the coefficient of restitution has been shown to decrease with increasing impact velocity (Goldsmith 1960; Johnson 1985).

The measurements made using the thin glass wall resulted in lower coefficients of restitution. With either a glass or steel impact particle, for the same velocity range, the average value of the coefficient of restitution was lower and the standard deviation was higher ( $\bar{e} = 0.88 \pm 0.07$ ). These lower values of the coefficient of restitution are in accordance with the measurements obtained by Goldsmith (1960) and Sondergaard *et al.* (1990). In those studies, the reduction of the coefficient of restitution was attributed

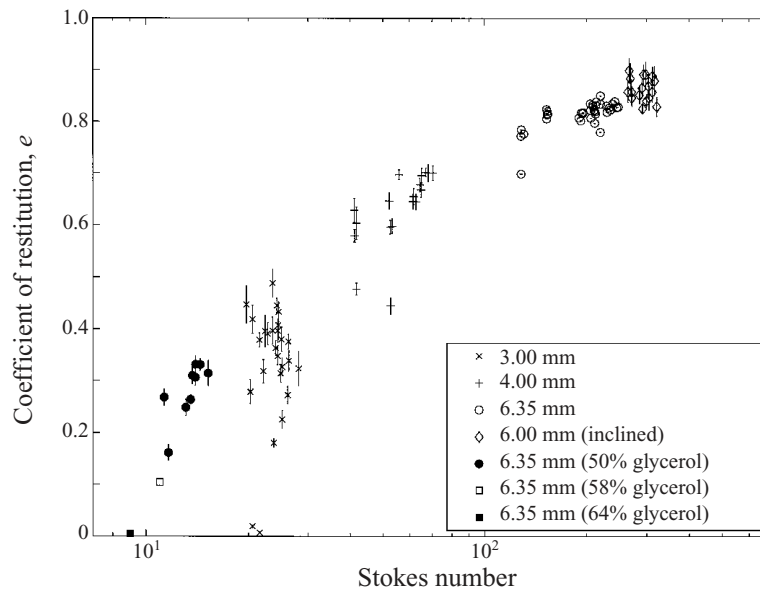


FIGURE 4. Coefficient of restitution,  $e$ , as a function of Stokes number for collisions with glass particles on the zerodur wall in water and glycerol-water mixtures.

to the wall thickness because the elastic waves generated by the particle collision were reflected to the impact point during the particle contact time.

### 3.2. Coefficient of restitution with fluid effects

Figure 4 shows the coefficients of restitution measured for the different glass impact particles on the zerodur wall in water, and glycerol in water mixtures, as a function of the impact Stokes number  $St$ . The data indicate that the coefficient of restitution increases with the Stokes number based on the impact velocity. The data show error bars that represent the correlation values of the line fits used to calculate the approach and rebound velocities. One of the data sets is taken with the zerodur wall inclined  $18^\circ$  with respect to the vertical such that at impact the particle is still accelerating; the data using the inclined wall are consistent with the other data sets. For the cases where the particle's position did not vary with time after impact a value of zero is assigned to the coefficient of restitution. Generally, for  $St$  less than 80, the scatter of the data is large and outside the error bars. A possible reason for the scatter is discussed in §4.1.

Figure 5 shows the measured coefficients of restitution as a function of the impact Stokes number for steel impact particles on the zerodur wall in several glycerol-water mixtures. The measured coefficients of restitution follow the same trend as in the experiments for the glass particles but the variance of the results is smaller.

Measurements were also obtained with the nylon and Delrin particles. The measurements obtained for collisions with these spheres in water on the zerodur wall are shown in figure 6, along with the measurements for glass and steel particles. Also included are the data for collisions of the glass sphere in air. The trend is the same for all the materials, regardless of the particle diameter and density. The Stokes number is the appropriate parameter to represent the results. Within experimental uncertainty, the data show the coefficient of restitution to be independent of the density ratio of the solid to fluid phases. For example, in the range of Stokes numbers

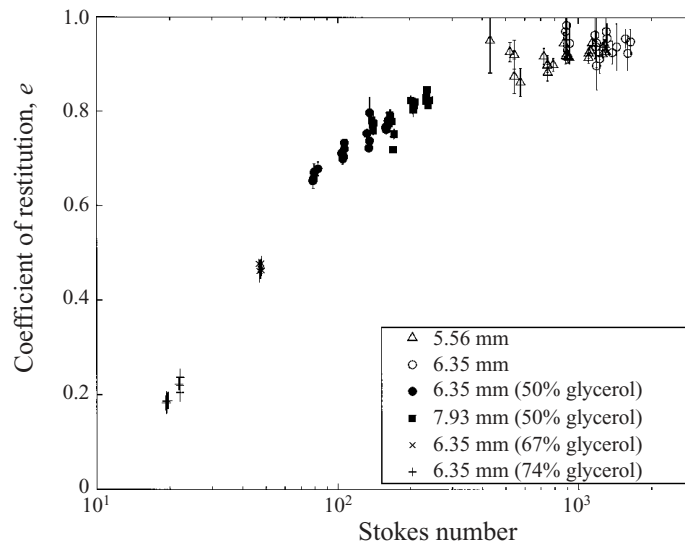


FIGURE 5. Coefficient of restitution,  $e$ , as a function of Stokes number for collisions with steel particles on the zerodur wall in water and glycerol–water mixtures.

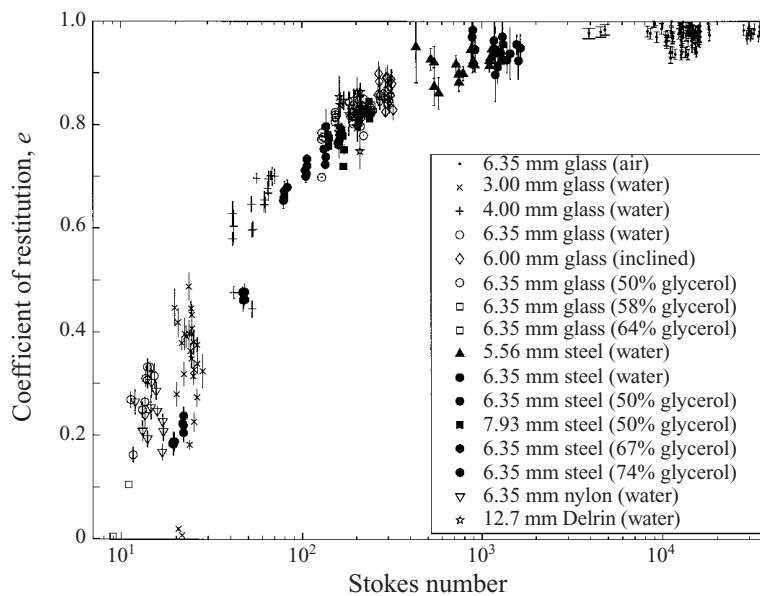


FIGURE 6. Coefficient of restitution,  $e$ , as a function of Stokes number for collisions of all particles with the zerodur wall in water.

between 100 and 300, the data for the 6.35 mm glass ( $\rho_p/\rho_f = 2.5$ ), for 12.7 mm Delrin ( $\rho_p/\rho_f = 1.4$ ) and for the 6.35 and 7.93 mm steel ( $\rho_p/\rho_f = 7.8$ ) appear to collapse to the same range of coefficients of restitution. The data also show that the coefficient of restitution is zero for Stokes numbers less than approximately  $St_c = 15$ .

In addition to the data using the zerodur wall, a Lucite wall was also used, and the results are presented in figure 7. Again, the data show that the coefficient of restitution depends on the impact Stokes number, and that the coefficient is zero for



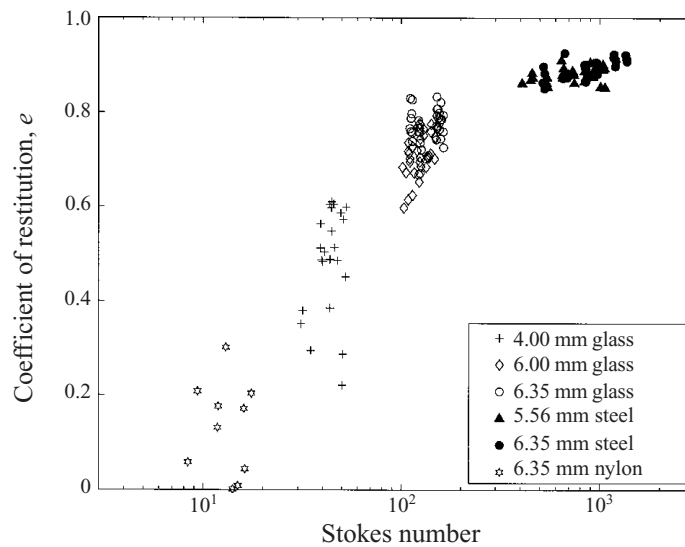


FIGURE 7. Coefficient of restitution,  $e$ , as a function of Stokes number for collisions with the Lucite wall in water.

Stokes numbers less than a critical value. In comparing the data for zerodur and Lucite walls, the coefficients of restitution for the Lucite appear to be slightly lower than those for the zerodur wall. This difference is also observed in the dry coefficient of restitution. A direct comparison between the data for collisions on zerodur and on Lucite is presented in §4.2.

Some data were also taken using the thin glass plate. Similarly to those found for the dry collisions, the data with the thin plate show a decrease in the average coefficient of restitution and a significant increase in scatter. At a Stokes number between 100 and 200, the average coefficient of restitution is 0.56, which is approximately 20% less than the value found using the zerodur wall. In addition, the standard deviation has increased to approximately  $\pm 0.10$ . The critical Stokes number also appears to be somewhat lower than for the zerodur wall.

Figure 8 shows the immersed collisions of steel particles on the zerodur wall, and also the measurements by McLaughlin (1968) and Gondret *et al.* (1999, 2000). The data compare well with the present measurements except for the values at high Stokes number by Gondret *et al.* (1999), which may be a result of the thin wall used in their experiments. These measurements seem to have been corrected in the later Gondret *et al.* (2000).

### 3.3. Approach of a particle to a wall

To quantify the effect of the wall on the trajectory of the particle a series of experiments was performed with a free swinging immersed pendulum. The trajectories for a particle colliding with the wall and for a free swinging particle were compared for the same particle and same initial release angle. The viscosity of the interstitial fluid was varied between 1 and  $12 \times 10^{-3}$  Pa s. Figure 9 shows the trajectories for five cases. The velocities have been non-dimensionalized by the velocity of the particle at a distance of 1.5 particle diameters from the wall. As seen in the figure, the velocity of the particle decreases due to viscous drag even before it reaches the vicinity of the wall. Note that when the wall is present there is a further reduction in the velocity of

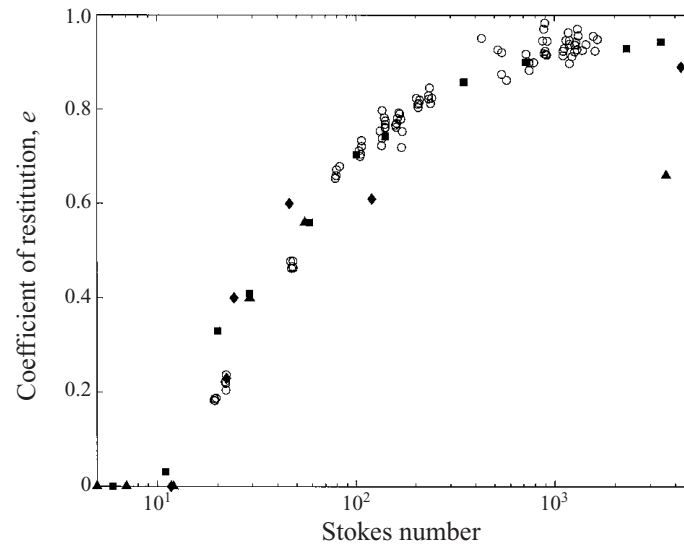


FIGURE 8. Coefficient of restitution,  $e$ , as a function of Stokes number for collisions with steel particles on a zerodur wall (○). Also shown are the results obtained by McLaughlin (1968) (◆), corresponding to steel ball bearings impacting an anvil, and by Gondret *et al.* (1999, 2000) (▲, ■), corresponding to steel spheres impacting a glass wall.

the particle as it approaches the wall. For  $St = 9$  based on the impact velocity, the particle starts decelerating at approximately 0.5 particle diameters from the wall, well ahead of the actual collision. This further reduction of the velocity is also noticeable for  $St = 13, 31,$  and  $47$ . By comparing the two trajectories, a distance,  $h_w$ , can be defined as a critical distance at which the velocity of the particle decreases due to the presence of the wall. The ratio of  $h_w$  to  $d$  is shown in figure 10, indicating a decrease in  $h_w/d$  with Stokes number. For  $St = 68$ , there is no apparent deceleration due to the presence of the wall. The seemingly low value of velocity for the last datum in figure 9(e) is a consequence of the numerical differentiation of the position data obtained from the high-speed video, as observed in figures 2 and 3. Figure 10 also shows the coefficient of restitution for the five experiments. Rebound did not occur for  $St = 9$ .

## 4. Discussion

### 4.1. Influence of the particle roughness

A distinctive feature of the measured coefficients of restitution is that the amount of variance increases as the impact Stokes number decreases. During the experiments, special care was taken to ensure that nominal conditions were kept constant for a given experimental set. The variance of the measured coefficient of restitution was observed to be larger than the experimental error for  $St$  less than 80 for experiments done with glass and nylon particles but was not observed in the experiments with steel particles. A possible difference between the types of particles involves the surface properties.

The surface roughness is quantified using two parameters as presented in table 1. The root-mean-square surface roughness, or standard deviation of the surface height,  $\sigma_s$ , describes the variation in surface elevation with respect to a flat or mean (reference)

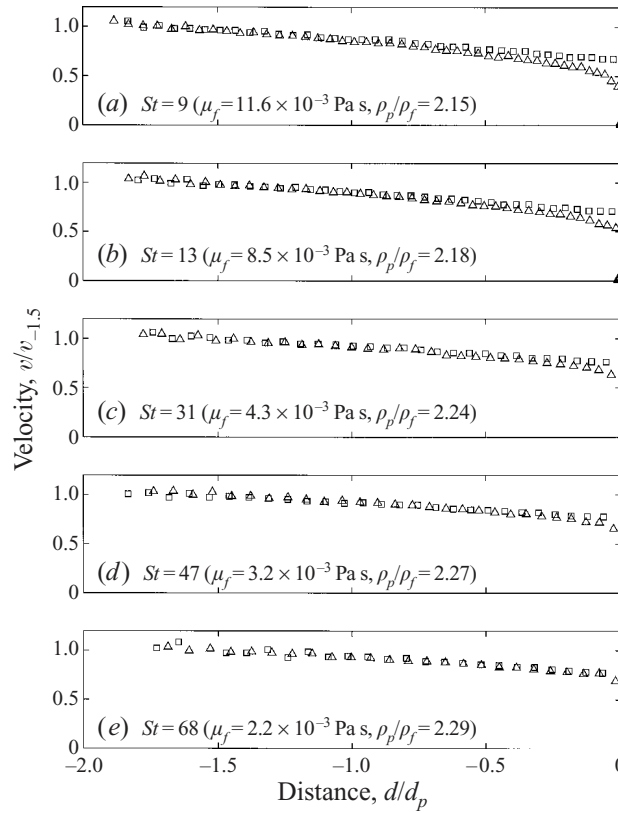


FIGURE 9. Comparison of the velocity–position plots for a particle colliding with a wall ( $\Delta$ ) and a free swinging pendulum ( $\square$ ). The subfigures correspond to the conditions indicated by the corresponding points in figure 10.

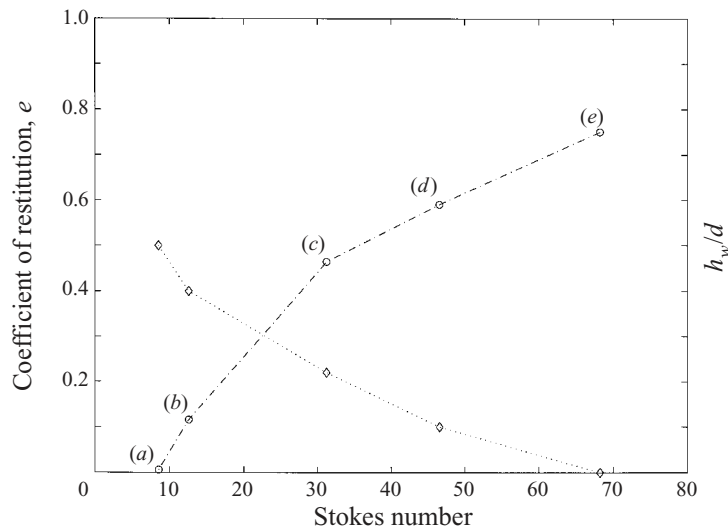


FIGURE 10. Coefficient of restitution ( $\circ$ ) and critical distance ( $\diamond$ ) corresponding to five trials with a 6.35 mm glass bead impacting a zerodur wall, immersed in glycerol–water mixtures with viscosities between (a)  $11.6 \times 10^{-3}$  Pa s and (e)  $2.2 \times 10^{-3}$  Pa s.

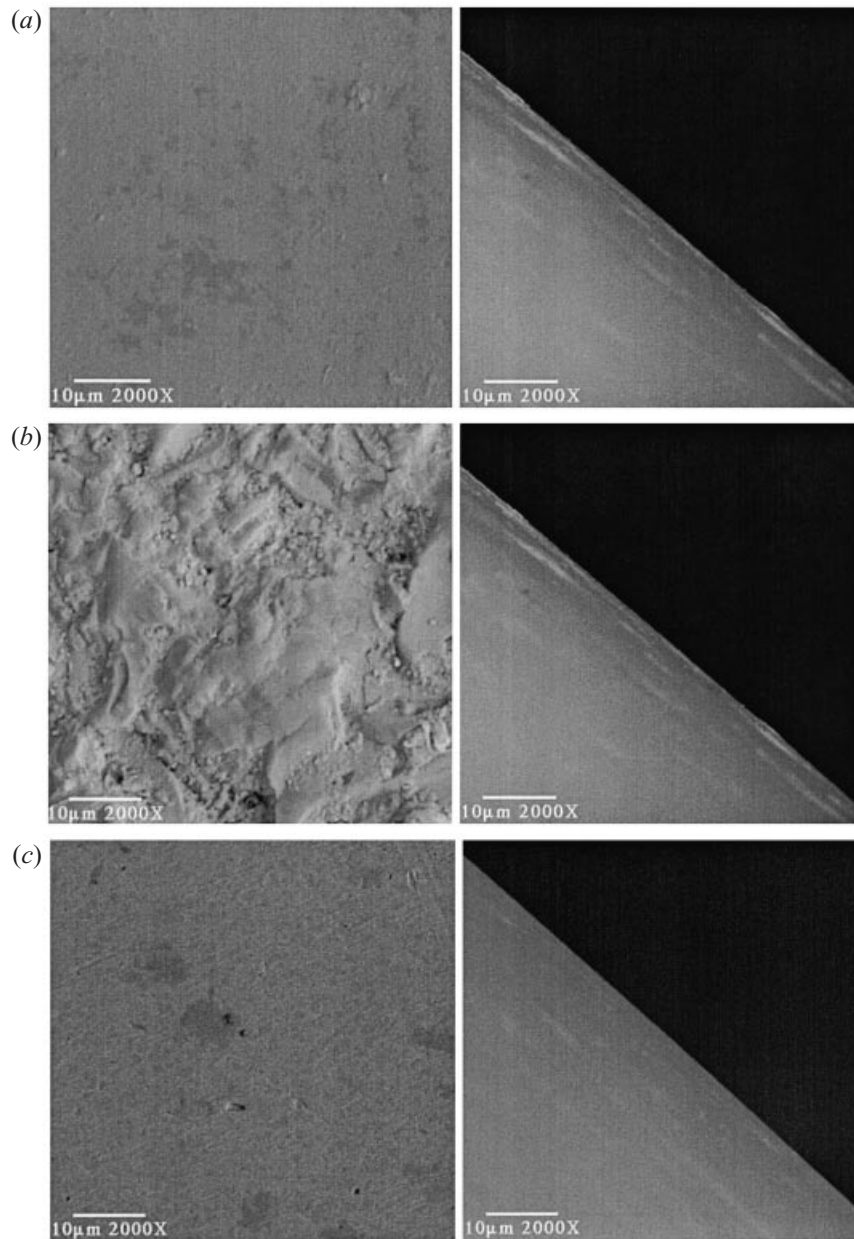


FIGURE 11 (a-c). For caption see facing page.

surface. In addition to  $\sigma_s$ , the profile of a random surface may be characterized by its autocorrelation function (Thomas 1999) that describes the similarity between the height,  $z$ , of the surface at some distance,  $x$ , along the surface. As the horizontal distance between two surface points increases, the autocorrelation function decreases toward zero since the correlation between the heights of those two surface points decreases. The maximum distance at which a significant correlation occurs is called the correlation length,  $\lambda_p$ , and is defined as the displacement for which the autocorrelation function is equal to  $e^{-1}$  ( $\sim 0.36788$ ).

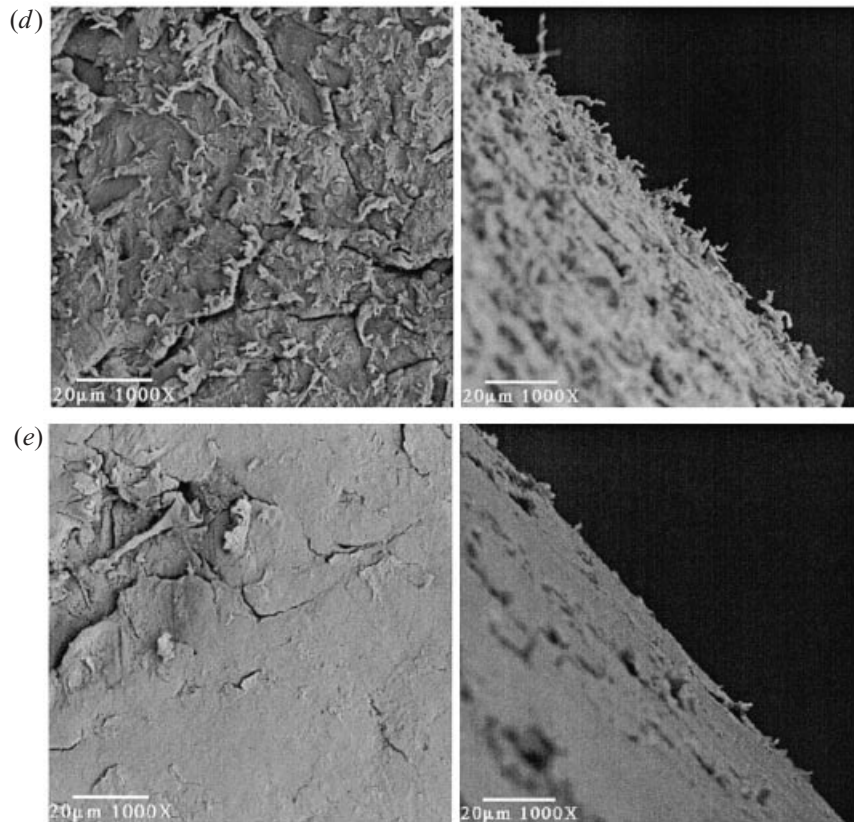


FIGURE 11. SEM photographs of the surfaces of the particles used in the experiments: (a) Glass bead, 6.00 mm,  $\times 2000$ ; (b) Glass sphere, 6.35 mm,  $\times 2000$ ; (c) Steel sphere, 6.35 mm,  $\times 2000$ ; (d) Nylon sphere, 6.35 mm,  $\times 1000$ ; (e) Delrin sphere, 12.70 mm,  $\times 1000$ .

Figure 11 shows scanning electron microscopy images of the surface of five typical particles used in these experiments. Figure 11(a) shows the structure of the surface of the glass bead that has solitary abrupt asperities with a fairly long correlation distance. In contrast, the ground glass spheres, shown in figure 11(b), have smoother asperities with a short correlation distance. The steel ball bearings are smooth with some isolated scratches along the surface, as shown in figure 11(c). The plastic spheres have both a large r.m.s. roughness and a long correlation distance. The nylon sphere, portrayed in figure 11(d), presents an intricate surface with filaments of material towering above the mean surface. The Delrin sphere, shown in figure 11(e), has a surface covered with a regular distribution of small Delrin flakes.

As a particle approaches the wall, Davis *et al.* (1986) predicted a closest distance of approach,  $h_m$ , which depends on the elasticity parameter  $\epsilon$  and the Stokes number. For the collisions in the present study, the scaled approach distance  $h_m/x_1$ , where  $x_1 = (40\mu w_0 a^{3/2})^{2/5}$ , varies from approximately 1/4 to 1/3 and is nearly independent of  $\epsilon$  and  $St$  for  $St$  greater than the critical value. Hence, it is possible to use the Davis *et al.* study to estimate the closest distance of approach for various collision conditions.

Calculated values of  $h_m = x_1/3$  are found in table 3 for experimental conditions

Material	$d_p$ (mm)	$v_0$ (mm s <sup>-1</sup> )	$\mu$ (Pa s)	$h_m$ ( $\mu\text{m}$ )	$\sigma_s/h_m$	$A_h$ ( $\mu\text{m}^2$ )	$\lambda_s$ ( $\mu\text{m}^2$ )	$A_h/\lambda_s$
Glass beads	3.0	25	0.001	0.0063	21.96	859.4	3595.9	0.239
	4.1	50	0.001	0.0100	5.02	2794.6	3034.3	0.921
Glass sphere	6.35	50	0.005	0.0243	5.37	6703.5	918.7	7.297
Steel	6.35	80	0.024	0.0449	0.53	12310.3	4153.4	2.964
	6.35	100	0.014	0.0396	0.60	14716.2	4153.4	3.543
Nylon	6.35	20	0.001	0.0276	72.88	6324.2	3154.2	2.005

TABLE 3. Typical collision parameters for  $St$  less than 80.

corresponding to  $St$  less than 80. These values are compared with the r.m.s. surface roughness,  $\sigma_s$ . As shown in the table, this comparison suggests that  $h_m$  is larger than  $\sigma_s$  only for the steel spheres; for the glass sphere and beads, and the nylon particle,  $\sigma_s$  is significantly larger than  $h_m$ . Also presented in table 3 is the contact area  $A_h = \pi r_h^2$  calculated from Hertzian contact theory (Goldsmith 1960), which predicts that the radius of the contact is given by

$$r_h = \left( \frac{3\pi}{8} \theta d_p F \right)^{1/3},$$

where  $F$  is the equivalent load due to the impact and is obtained from

$$F = \frac{d_p^2}{3\pi\theta} \left( \frac{5\pi^2}{4} \rho_p \theta u_i^2 \right)^{3/5}.$$

This area is compared with an average roughness area  $\lambda_s = 1.8\lambda_p^2$ . Over a wide range of finite sampling intervals  $\lambda_s$  is the area in which, on average, one asperity can be found (Johnson 1985). Hence, the ratio of the Hertzian contact area to the roughness correlation area increases as the number of asperities involved in a contact event increases.

An explanation for the variation in the measured coefficients of restitution involves these two ratios. For the steel particles, the  $\sigma_s$  is smaller than the calculated distance  $h_m$  and the effective contact area is larger than  $\lambda_s$ . For these conditions, the variability from collision to collision is expected to be small, which is consistent with the repeatable results for the steel particles shown in figure 6. When the  $h_m$  is smaller than the  $\sigma_s$  and the effective collision area is much larger than  $\lambda_s$ , such as for the glass sphere or the nylon particle, the particle and surface may interact through the tops of the asperities. Although the fluid may still lubricate the surface of the asperities, the asperities differ in size and orientation, which may contribute to the scatter in the data. In addition, the fluid trapped in the crevices may change pressure as it is compressed. As a result, the rebound velocity may be more variable from experiment to experiment. When  $h_m$  is smaller than  $\sigma_s$  and the effective collision area is smaller than  $\lambda_s$ , the roughness may or may not be directly involved in a given collision. Hence, for the small glass beads the variability in the rebound velocity may result from relatively large asperities being contacted on an irregular basis.

As the particle velocity is increased,  $h_m$  increases; in addition, the Hertzian contact area also increases. Both of these effects may contribute to the smaller scatter found at higher Stokes numbers. In addition, the rebound of the particle at low velocities may be affected by other factors. Even though great care is taken in maintaining the experimental conditions as constant as possible, any asymmetry in the release

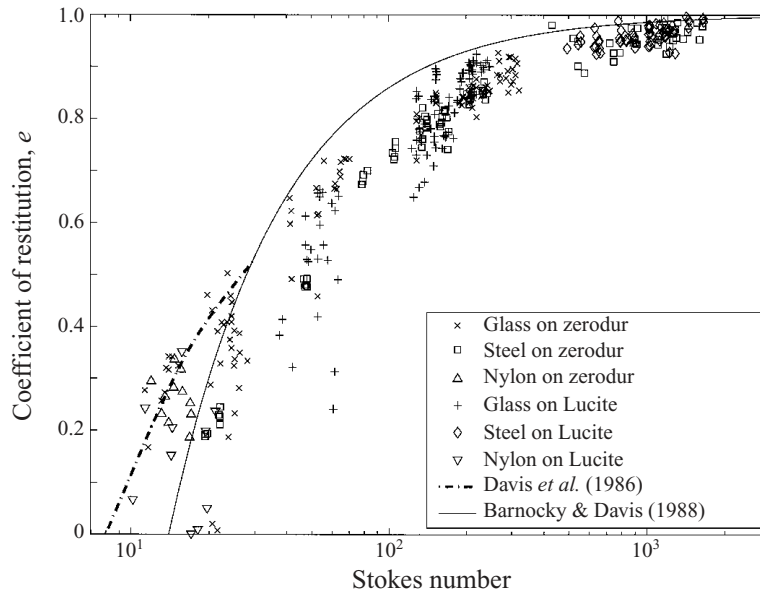


FIGURE 12. Effective coefficient of restitution,  $e$ , scaled by the dry coefficient of restitution,  $e_{dry}$ , as a function of Stokes number for immersed particle–wall collisions. The dashed–dotted line shows the coefficient of restitution from the calculations by Davis *et al.* (1986) for a value of the elasticity parameter  $\epsilon \approx 10^{-8}$ . The solid line shows the coefficient of restitution from the calculations by Barnocky & Davis (1988) for  $e_{dry} = 0.98$  and  $x_c/x_0 = 10^{-3}$ .

of the bead may cause a slight spin along the axis of the string of the pendulum. Consequently, the local asperities involved in a particular collision may be different from the ones involved in a subsequent collision, adding to the dispersion of the data.

#### 4.2. Comparison with elastohydrodynamic theories

Since the rebound velocity depends on the elastic properties of the materials, the experiments done with the zerodur and Lucite walls were compared. The coefficients of restitution for the Lucite were found to be slightly lower than those for the zerodur wall. If the results for the two walls are presented as a ratio of the immersed and dry coefficients of restitution, the results compare well, as shown in figure 12.

Following the analysis proposed by Davis *et al.* (1986), the viscous component of the coefficient of restitution for an immersed collision can be obtained. Davis *et al.* performed calculations to predict the maximum rebound velocity of elastic particles colliding in a viscous fluid. They characterized the collisions with two parameters, the particle Stokes number and an elasticity parameter,  $\epsilon$ , defined in §1. For the experiments performed in this study the values of  $\epsilon$  ranged from  $10^{-7}$  to  $10^{-8}$ . The predictions by Davis *et al.* for a value of  $\epsilon = 10^{-8}$  were used such that comparisons could be drawn between their calculations and the present measurements. The dashed–dotted line in figure 12 shows this prediction indicating the sharp increase in  $e$  as  $St$  increases from the critical value. Predictions for  $\epsilon = 10^{-7}$  would result in slightly higher values of  $e$  than those for  $\epsilon = 10^{-8}$ . It is important to note that the Davis *et al.* study predicted that the two surfaces would not come into contact and that the rebound results from the stored elastic energy. The present comparison suggest that the elastohydrodynamic theory may be extended to slightly inelastic surfaces by normalizing the results with the values for dry collisions.

A different method of obtaining the coefficient of restitution for an immersed collision was proposed by Barnocky & Davis (1988). The model is based on the assumption that the lubrication approximation breaks down at a critical distance, comparable to the size of the roughness of the particle surfaces.

From lubrication theory, the hydrodynamic force exerted on a sphere approaching a wall is

$$F_{drag} = 6\pi\mu a u \frac{a}{x} = -m \frac{du}{dt}, \quad (4.1)$$

where  $x$  is the gap between the surface of the particle and the wall. To estimate the viscous dissipation produced by a particle colliding with and rebounding from a wall, the equation of motion is integrated in two parts. The first (approach) portion is evaluated from  $x_0$  to the critical distance,  $x_c$ , at which the lubrication approximation breaks down due to surface roughness. The second part (rebound portion) is calculated from  $x_c$  back to  $x_0$ , in order to obtain the total velocity decay.

For the approach, a collision velocity,  $u_c = u(x = x_c)$ , is obtained,

$$\frac{u_c}{u_0} = 1 + \frac{1}{St_0} \ln \frac{x_c}{x_0}, \quad (4.2)$$

where  $St_0$  is the particle Stokes number at  $x_0$ . The velocity after impact is taken as  $e_{dry}u_c$ , which accounts for the solid–solid contact. Therefore, the rebound velocity of the particle as it returns to  $x_0$  is

$$\frac{u_r}{u_0} = e_{dry} \frac{u_c}{u_0} + \frac{1}{St_0} \ln \frac{x_c}{x_0} = e_{x_0}. \quad (4.3)$$

Note that  $u_r/u_0$  is a coefficient of restitution,  $e_{x_0}$ , defined at a position  $x_0$ , that accounts for losses within the lubrication layer and due to solid–solid contact. Hence, this effective coefficient of restitution is found to be

$$e_{x_0} = e_{dry} + \frac{1 + e_{dry}}{St_0} \ln \frac{x_c}{x_0}, \quad (4.4)$$

where  $x_c/x_0$  can be estimated from the physical variables of the problem. Considering a typical value of surface roughness in the order of  $0.1 \mu\text{m}$  and assuming  $x_0 = a/100$ , a value of  $x_c/x_0$  is approximately  $10^{-3}$ . The solid line in figure 12 shows the comparison between the prediction from equation (4.4) for  $e_{dry} = 0.98$  and  $x_c/x_0 = 10^{-3}$  and the experimental measurements. It is important to note that the mechanics of the flow in the gap between the particle and the wall may be significantly affected by the presence of asperities on the surface of the particle. Hence, the dry coefficient of restitution may not capture all the losses associated with the solid–solid contact. In addition, the model assumes that the Stokes drag law is valid for the whole range of experiments. Still, this simple model compares qualitatively well with the experimental measurements. The rapid change of the coefficient of restitution is captured by the model for small values of Stokes number. However, the model predicts that the critical Stokes number at which rebound first occurs is higher for lower values of the dry coefficient of restitution, which seems to be inconsistent with the experiments. For higher values of the Stokes number the model underestimates the fluid dissipation occurring during the collision but predicts well the weak dependence of the coefficient of restitution for higher values of the Stokes number.



## 5. Summary

The experimental measurements show the dependence of the coefficient of restitution on the Stokes number. The coefficient of restitution increases with increasing Stokes number beyond a certain critical value of approximately 10. The elastic properties of the particles and the walls do not have a significant impact on the measured coefficients. However, if the wall is not of sufficient size, the coefficient of restitution is reduced and the scatter in the measurements is increased. These results compare well with experimental studies in the literature.

A deceleration of the particles due to the presence of the wall was observed for collisions at Stokes numbers lower than approximately 70. The distance from the wall at which the particle starts decelerating increases with decreasing Stokes number. For a Stokes number of 9 the approach is affected at a distance of approximately one particle radius.

The analysis proposed by Davis *et al.* (1986), which predicts a rapid increase of the coefficient of restitution for low Stokes numbers, compared well with the measurements when presented as a ratio of the immersed and dry coefficients of restitution. Based on this analysis and on the surface properties of the particles, an explanation of the variance of the data is proposed. A simple analytical model based on Barnocky & Davis (1988) also compared favourably with the experimental data. The characteristic variance observed in the measurements of the immersed coefficients of restitution for  $St$  less than 80 appears to be a consequence of the interaction of the roughness of the surfaces with the fluid trapped between them. The variance is of the order of the experimental uncertainty for smooth particles and considerably larger for the rougher particles.

G.G.J. acknowledges financial support from Universidad Nacional Autónoma de México, through the Dirección General de Apoyo al Personal Académico, and through the Instituto de Investigaciones en Materiales. A.M.R. thanks Dr and Mrs Thomas J. Tyson for supporting him as a Howel N. Tyson SURF Fellow. We are grateful to Professor Paul C. Jennings for providing the zerodur block used in the present study and to Philippe Gondret for the preprint of the paper by his group. This work is supported by the National Science Foundation under grants CTS-9530357 and CTS-9908430.

## REFERENCES

- BARNOCKY, G. & DAVIS, R. H. 1988 Elastohydrodynamic collision and rebound of spheres: experimental verification. *Phys. Fluids* **31**, 1324–1329.
- BARNOCKY, G. & DAVIS, R. H. 1989 The influence of pressure-dependent density and viscosity on the elastohydrodynamic collision and rebound of two spheres. *J. Fluid Mech.* **209**, 501–519.
- BRENNER, H. 1961 The slow motion of a sphere through a viscous fluid towards a plane surface. *Chem. Engng Sci.* **16**, 242–251.
- DAVIS, R. H., SERAYSSOL, J. M. & HINCH, E. J. 1986 The elastohydrodynamic collision of 2 spheres. *J. Fluid Mech.* **163**, 479–497.
- FOERSTER, S. F., LOUGE, M. Y., CHANG, A. H. & ALLIA, K. 1994 Measurements of the collision properties of small spheres. *Phys. Fluids* **6**, 1108–1115.
- GLOWINSKI, R., PAN, T. W., HESLA, T. J. & JOSEPH, D. D. 1999 A distributed Lagrange multiplier fictitious domain method for particulate flows. *Intl J. Multiphase Flow* **25**, 755–794.
- GOLDSMITH, W. 1960 *Impact*. London: Edward Arnold (Publishers) Ltd.
- GONDRET, P., HALLOUIN, E., LANCE, M. & PETIT, L. 1999 Experiments on the motion of a solid sphere toward a wall: From viscous dissipation to elastohydrodynamic bouncing. *Phys. Fluids* **11**, 2803–2805.

- GONDRET, P., LANCE, M. & PETIT, L. 2000 Bouncing motion of spherical particles in fluids. *Phys. Fluids* Under consideration for publication.
- HU, H. H. 1996 Direct simulation of flows of solid-liquid mixtures. *Intl J. Multiphase Flow* **22**, 335–352.
- JOHNSON, K. L. 1985 *Contact Mechanics*. Cambridge University Press.
- KYTOMAA, H. & SCHMID, P. 1992 On the collision of rigid spheres in a weakly compressible fluid. *Phys. Fluids A* **4**, 2683–2689.
- LUNDBERG, J. & SHEN, H. 1992 Collisional restitution dependence on viscosity. *J. Engng Mech. Div. ASCE* **118**, 979–989.
- MCLAUGHLIN, M. H. 1968 An experimental study of particle-wall collision relating of flow of solid particles in a fluid. Engineer's degree thesis, California Institute of Technology, Pasadena, California.
- SMART, J. R. & LEIGHTON, D. T. 1989 Measurement of the hydrodynamic surface-roughness of noncolloidal spheres. *Phys. Fluids A* **1**, 52–60.
- SONDERGAARD, R., CHANEY, K. & BRENNEN, C. E. 1990 Measurements of solid spheres bouncing off flat plates. *Trans. ASME: J. Appl. Mech.* **57**, 694–699.
- THOMAS, T. R. 1999 *Rough Surfaces*, 2nd edn. Imperial College Press.
- ZENIT, R. & HUNT, M. L. 1999 Mechanics of immersed particle collisions. *Trans. ASME: J. Fluid Engng* **121**, 179–184.